

Effect of cobalt substitution on magneto-transport properties of Nd 0.7 Sr 0.3 Mn 1 x Co x O 3 (0.0 x 1)

Saket Asthana, A. K. Nigam, and D. Bahadur

Citation: *Journal of Applied Physics* **97**, 10C101 (2005); doi: 10.1063/1.1845952

View online: <http://dx.doi.org/10.1063/1.1845952>

View Table of Contents: <http://scitation.aip.org/content/aip/journal/jap/97/10?ver=pdfcov>

Published by the [AIP Publishing](#)

Articles you may be interested in

[Magnetic and transport properties of cobalt doped La_{0.7}Sr_{0.3}MnO₃](#)

J. Appl. Phys. **116**, 103907 (2014); 10.1063/1.4894713

[Tunable spin reorientation transition and magnetocaloric effect in Sm_{0.7-x}La_xSr_{0.3}MnO₃ series](#)

J. Appl. Phys. **113**, 013911 (2013); 10.1063/1.4773337

[Electrical transport properties and magnetic cluster glass behavior of Nd 0.7 Sr 0.3 Mn O 3 nanoparticles](#)

J. Appl. Phys. **100**, 104318 (2006); 10.1063/1.2387056

[Magnetoelastic effects of \(La 1-x Gd x \) 0.7 Ca 0.3 MnO 3 \(x=0,0.05,0.2,0.3 ,and 0.4\) compound](#)

J. Appl. Phys. **93**, 1142 (2003); 10.1063/1.1531213

[Curie temperature of Nd 0.7 \(Ca,Sr,Ba \) 0.3 MnO 3 , as determined by electron-spin resonance](#)

J. Appl. Phys. **89**, 3377 (2001); 10.1063/1.1348325



Not all AFMs are created equal
Asylum Research Cypher™ AFMs
There's no other AFM like Cypher

www.AsylumResearch.com/NoOtherAFMLikeIt

OXFORD
INSTRUMENTS
The Business of Science®

Effect of cobalt substitution on magneto-transport properties of $\text{Nd}_{0.7}\text{Sr}_{0.3}\text{Mn}_{1-x}\text{Co}_x\text{O}_3$ ($0.0 \leq x \leq 1$)

Saket Asthana

Metallurgical Engineering and Materials Science, Indian Institute of Technology, Bombay, Mumbai 400076 India

A. K. Nigam

Tata Institute of Fundamental Research, Colaba, Mumbai 400005 India

D. Bahadur^{a)}

Metallurgical Engineering and Materials Science, Indian Institute of Technology, Bombay, Mumbai 400076 India

(Presented on 9 November 2004; published online 4 May 2005)

Magnetic and transport studies of the compounds $\text{Nd}_{0.7}\text{Sr}_{0.3}\text{Mn}_{1-x}\text{Co}_x\text{O}_3$ ($0.0 \leq x \leq 1$) have been carried out. The compositions crystallize in single-phase ortho-perovskite. The conduction mechanism could be explained using the small polaron correlated hopping model. The thermal irreversibility in zero-field and field-cooled magnetization data increases with Co content, which is due to the different spin states of the Co. Transition of Co^{3+} from high spin/intermediate spin to low spin state is observed at low temperatures. The nonsaturating M - H behavior is observed in cobalt containing samples due to suppression of double-exchange interaction which favors long-range ferromagnetic order. © 2005 American Institute of Physics. [DOI: 10.1063/1.1845952]

I. INTRODUCTION

The hole-doped manganites $\text{Ln}_{1-x}\text{A}_x\text{MnO}_3$ have been studied extensively since the discovery of colossal magnetoresistance (CMR).¹ The average A-site ionic radius, size variance, and mixed valence state in the manganites affect the magnetic and magneto-transport properties. The partial substitution of rare earth ion by bivalent cations leads to the existence of mixed valence state of Mn^{3+} and Mn^{4+} ions, which facilitates the double-exchange (DE) interaction responsible for CMR behavior. Although extensive work has been done on B-site substitution, the work of Co substitution on Mn site is limited.²

It is well established that cobalt exhibits different spin states.^{3,4} The low spin (LS, $t_{2g}^6 e_g^0$) state changes to either high spin (HS, $t_{2g}^4 e_g^2$) or intermediate spin (IS, $t_{2g}^5 e_g^1$) states with increasing temperature. In the present work, we have studied the effect of cobalt (Co) substitution on Mn site for the series $\text{Nd}_{0.7}\text{Sr}_{0.3}\text{Mn}_{1-x}\text{Co}_x\text{O}_3$ ($0 \leq x \leq 1$).

II. EXPERIMENTAL DETAILS

Polycrystalline samples of the series $\text{Nd}_{0.7}\text{Sr}_{0.3}\text{Mn}_{1-x}\text{Co}_x\text{O}_3$ ($0 \leq x \leq 1$) were synthesized through citrate gel route. The as-prepared powders were calcined at 1200 °C in air for 6 h. The powders were pelletized in the form of rectangular bars and sintered at 1300 °C in air for 4 h. X-ray diffraction patterns of the samples were recorded using $\text{Cu-K}\alpha$ radiation (PANalytical, PW 3040/60 Philips). Resistivity measurements at different applied magnetic fields were carried out between 20 and 320 K using the standard four-probe dc method. Magnetic measurements were made

using a vibrating sample magnetometer (VSM, Oxford) at different fields and in the temperature range 5 to 300 K.

III. RESULTS AND DISCUSSION

The samples of the series are indexed with orthorhombic structure. The tolerance factor (t), which is the ratio of A–O and B–O bond distances in the ABO_3 perovskite, vary from 0.9171 (for $x=0$) to 0.9284 (for $x=1$). The splitting in the high-angle peaks is observed with Co content due to increasing tolerance factor which is attributed to the structural transition from $Pnma$ ($x=0$) to $Imma$ ($x=1$).

Figure 1 shows temperature dependence of magnetization in a field of 0.01 T. The thermo-magnetic irreversibility behavior in zero-field cooled (ZFC) and field cooled (FC) is observed in all the samples. This may be observed due to the frustration caused by competing superexchange (SE) and DE interactions. The DE interaction is stronger for

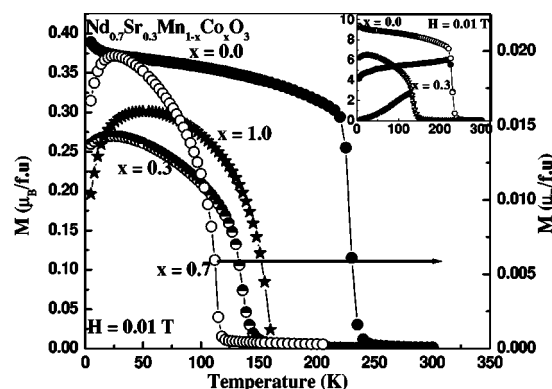


FIG. 1. Temperature dependence of magnetization in a field of 0.01 T for $\text{Nd}_{0.7}\text{Sr}_{0.3}\text{Mn}_{1-x}\text{Co}_x\text{O}_3$ ($x=0, 0.3, 0.7,$ and 1) compounds. Thermal irreversibility behavior is shown in the inset.

^{a)}Electronic mail: dhiren@met.iitb.ac.in

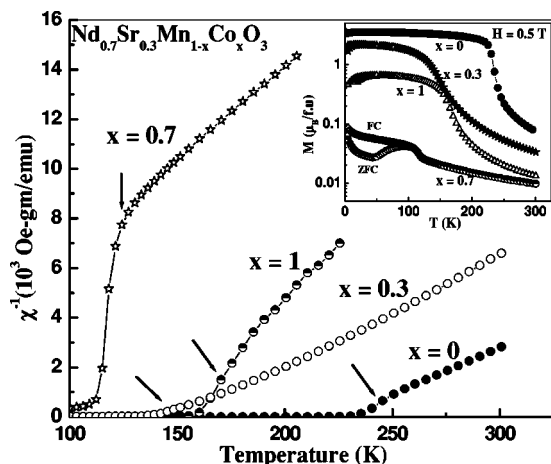


FIG. 2. Variation of inverse susceptibility with temperature for $\text{Nd}_{0.7}\text{Sr}_{0.3}\text{Mn}_{1-x}\text{Co}_x\text{O}_3$ ($x=0, 0.3, 0.7$, and 1) compounds. The HS/IS to LS transition temperature is indicated by arrows. Inset shows the $M(T)$ behavior in 0.5 T field.

$\text{Mn}^{3+}-\text{O}^{2-}-\text{Mn}^{4+}$ in comparison to that of $\text{Co}^{3+}-\text{O}^{2-}-\text{Co}^{4+}$.² The strong irreversibility shown in the inset of Fig. 1 (particularly for sample with $x=0.3$) is characteristic of highly anisotropic compounds. Hence, the large anisotropy may be on account of Nd^{3+} ion with a large orbital angular momentum (L) value of 6 and intermediate spin (IS) state of Co^{3+} ($t_{2g}^5e_g^1$), which is a Jahn–Teller (JT) ion. The larger spin-orbit coupling due to these ions and JT distortion plays a significant role.

The gradual decrease in peak magnetization is observed with increasing Co content. All the samples exhibit the paramagnetic (PM) to ferromagnetic (FM) transition at a characteristic temperature T_C . The FM to AFM transition is observed only in Co containing samples at critical temperature T_N , at which Co presumably changes from IS to LS state. T_C and T_N are determined by the maximum and minimum, respectively, in dM/dT plots. In Nd compound Co^{3+} ions remain in low spin over a large temperature range as compared to La compound due to the greater acidity of the Nd^{3+} with respect to La^{3+} , which causes an increase in the crystal-field splitting.⁵ None of the samples follow the Curie–Weiss behavior, which indicates the presence of microscopic magnetic inhomogeneities as shown in Fig. 2. The deviation from the linearity in inverse susceptibility versus temperature plot suggests that the cobalt HS(or IS) state changes to LS state below a critical temperature. The HS(IS) to LS transition temperature (T_L) for the mother compound ($x=1$) is ~ 170 K compared to ~ 250 K (Ref. 5) for NdCoO_3 compound, which could be due to variation in crystal-field splitting Δ_{cf} . Except for the sample with $x=0.7$, all others approach near saturation in a field of 0.5 T as shown in the inset of Fig. 2. The magneto-thermal irreversibility behavior decreases in 0.5 T field. The FC plot for sample with $x=0.7$ gives a small magnetic moment of $0.08 \mu_B/\text{f.u.}$ as compared to $3.52 \mu_B/\text{f.u.}$ for $x=0$ sample. This is presumably due to higher percentage of Co^{4+} which causes frustration at low temperatures.

Figure 3 shows the isothermal magnetization plots for $x=0.3, 0.7$, and 1.0 samples at 5 K. None of these samples shows saturation even up to a field of 6 T. The sample with

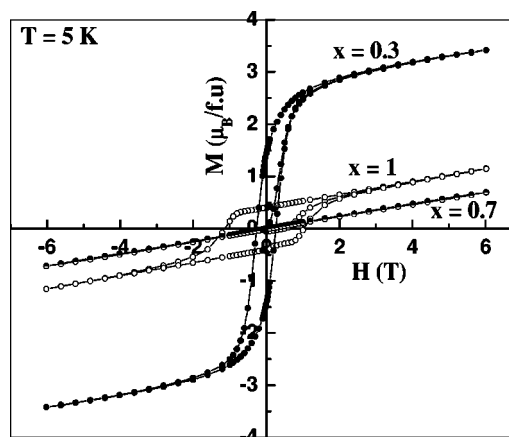


FIG. 3. Isothermal magnetization plots for $\text{Nd}_{0.7}\text{Sr}_{0.3}\text{Mn}_{1-x}\text{Co}_x\text{O}_3$ ($x=0.3, 0.7$, and 1) compounds at 5 K.

$x=1$ shows the prominent hysteresis behavior. No hysteresis is observed for sample with $x=0.7$ and the magnetic moment is the lowest ($0.7 \mu_B/\text{f.u.}$) as compared to that $3.42 \mu_B/\text{f.u.}$ of $x=0.3$ sample. The sample with $x=0.3$ and 1 shows large hysteresis (high coercivity, H_c) values of 0.25 and 1.2 T, respectively. Except for $x=1$, the nonsaturating $M-H$ behavior in all the cases could be explained on the basis of competing DE and SE interactions. DE alone is not responsible for the nonsaturating $M-H$ behavior in the case of $x=1$ sample due to the absence of strong Hund's coupling. This behavior could be explained on the basis of an increased anisotropy of the FM character, which arises due to the presence of orbital moments of (IS) Co and Nd^{3+} ions.^{6,7} The large coercivity of 1.2 T for the sample with $x=1$ also indicates that the Co ion (IS) and Nd^{3+} ($L=6$) induce a large anisotropy.

The temperature dependence of resistivity behavior for samples with $x=0, 0.1$, and 0.3 is shown in Fig 4. The resistivity data for the compositions $x \geq 0.5$ were beyond the measurement limit of the instrument. The semiconducting behavior of the sample with $x=1$ is already reported.⁸ The ratio of $\text{Mn}^{3+}/\text{Mn}^{4+}$ decreases with Co content, increasing $\text{Co}^{3+}/\text{Co}^{4+}$ ratio. The metal insulator (MI) transition is observed only in the sample with $x=0$ at 238 K. The resistivity

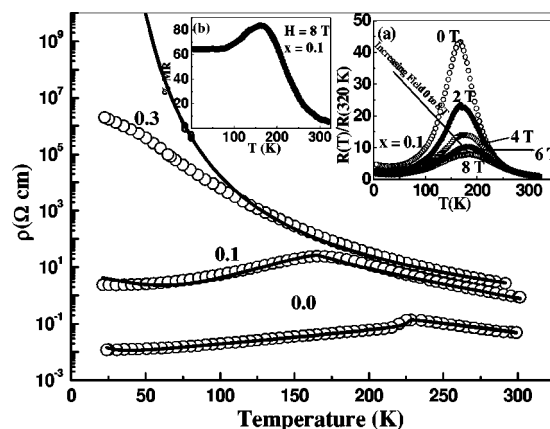


FIG. 4. Variation of resistivity with temperature for the samples with $x=0, 0.1$, and 0.3 . Lines show the theoretical fitted plots. Inset shows the effect of magnetic field on resistance for the sample with $x=0.1$.

TABLE I. Parameters used to fit the $\rho(T)$ data for the series $\text{Nd}_{0.7}\text{Sr}_{0.3}\text{Mn}_{1-x}\text{Co}_x\text{O}_3$ ($0.00 \leq x \leq 1$). The phonon frequency $\nu_{ph} = 5 \times 10^{12}$ Hz and $a = 3.858$ Å has been taken. “ n ” is the number of charge carries, ε_p is the value of small polaron stabilization energy, T_{ca} is an atomic ordering temperature, and U_0 is the activation energy. The values of tolerance factor (t), T_{MI} , T_C , T_N , T_L and the maximum magnetization (M_m) in a field of 0.5 T are also summarized.

x	t	T_{MI} (K)	T_C (K)	M_m $\mu_B/f.u$	T_L (K)	T_N (K)	n ($\times 10^{19}/\text{cm}^3$)	ε_p (K)	U_0 (K)	T_{ca} (K)
0.0	0.9171	238	230	3.52	~ 250	...	48.1	60	350	270
0.3	0.9204	...	140	2.18	155	23	10.22	680	700	350
0.7	0.9249	...	115	0.08	125	25
1.0	0.9284	...	160	0.66	170	50

values increase as the concentration of cobalt ion increases due to suppression of DE that leads to ferromagnetism. The population of Co (IS) changes to LS state at low temperatures, which creates an additional distortion in the lattice due to the smaller ionic size of the low spin Co^{3+} ion. As a result, buckling of CoO_6 octahedra increases, which in turn affects the charge transfer integral along the Co–O–Co bonds.⁶ This effect is probably the reason for monotonous increase in the resistivity behavior of the Co-containing samples. The resistivity data have been understood using the correlated small polaron-hopping model discussed in detail elsewhere.⁹ To fit the resistivity data for the sample with $x=0, 0.1$, and 0.3 , we have used $S_a^2=1$, $\sigma_a^2=(1-0.75 t_{ca}^3)^{1/2}$. The chemical and fitted parameters for this series of compounds are summarized in Table I.

The spin–spin scattering increases as the concentration of Co increases. The activation energy for polaron hopping as well as small polaron stabilization energy is high in the case of Co-substituted system. The number of charge carriers decreases with increasing Co content, as a result of which resistivity values increase. The sudden jump in the activation energy U_0 (350 to 700 K) and small polaron stabilization energy ε_p (60 to 680 K) is observed in Co-substituted sample. The Co substitution suppresses the DE interactions; hence, the higher activation energy is required for hopping of the e_g electrons.

The inset (a) of Fig. 4 shows the plot of normalized resistance versus temperature for varying magnetic fields for the sample with $x=0.1$. The T_{MI} shifts to higher temperature from 168 K (in 0 T) to 184 K (in 8 T). The peak in MR is observed at T_{MI} and its value is $\sim 85\%$ in 8 T field for $\text{Nd}_{0.7}\text{Sr}_{0.3}\text{Mn}_{0.9}\text{Co}_{0.1}\text{O}_3$ as shown in inset (b) of Fig. 4. The samples with $x=0.3$ and 0.7 and 1 show insignificant change in resistance with applied field due to their highly resistive behavior over the entire temperature range. The observation of nearly temperature-independent MR behavior at low temperatures may possibly be due to intergrain tunneling of spin-polarized carriers in applied magnetic field.

IV. CONCLUSIONS

All the samples of the series $\text{Nd}_{0.7}\text{Sr}_{0.3}\text{Mn}_{1-x}\text{Co}_x\text{O}_3$ ($0 \leq x \leq 1$), crystallized in orthorhombic structure. The magneto-thermal irreversibility in $M(T)$ data increases with Co content due to the HS (or IS) state to LS state transition. The large coercivity and thermal irreversibility are attributed to the anisotropic nature arising due to Co(IS) state, which is a JT ion and Nd^{3+} ion with a large orbital moments. The nonsaturating $M-H$ behavior is due to the competing DE and SE interactions and large anisotropy. The resistivity values increase with the cobalt concentration. The conduction mechanism could be understood by small polaron-correlated hopping model. The intergrain tunneling mechanism is presumably responsible for high MR behavior at low temperature. Overall magnetic as well as transport properties could be attributed to the HS/IS to LS transition in cobalt ion and high orbital contribution due to Nd^{3+} ion.

ACKNOWLEDGMENT

Two of the authors, S.A. and D.B., are thankful to the Department of Science and Technology (DST) India, for support of the project.

¹C. N. R. Rao and B. Raveau, *Colossal Magneto-resistance, Charge Ordering and Related Properties of Manganese Oxides* (World Scientific, Singapore: 1998).

²C. M. Srivastava, S. Banerjee, T. K. GunduRao, A. K. Nigam, and D. Bahadur, *J. Phys.: Condens. Matter* **15**, 2375 (2003).

³D. Bahadur, S. Kollali, C. N. R. Rao, M. J. Patni, and C. M. Srivastava, *J. Phys. Chem. Solids* **40**, 981 (1979).

⁴M. A. Korotin, S. Y. Ezhov, I. V. Solovyev, V. I. Anisimov, D. I. Khomskii, and G. A. Sawatzky, *Phys. Rev. B* **54**, 5309 (1996).

⁵G. Demazeau, M. Pouchard, and P. Hagenmuller, *J. Solid State Chem.* **9**, 202 (1974).

⁶M. Paraskevopoulos, J. Hemberger, A. Krimmel, and A. Loidl, *Phys. Rev. B* **63**, 224416 (2001).

⁷R. Ganguly, A. Maignana, M. Hervieu, C. Martin, and B. Raveau, *Solid State Commun.* **121**, 537 (2002).

⁸A. Fondado, M. P. Breijo, C. Rey-Cabezudo, M. Sanchez-Andujar, J. Mira, J. Rivas, and M. A. Senaris-Rodriguez, *J. Alloys Compd.* **323–324**, 444 (2001).

⁹C. M. Srivastava, *J. Phys.: Condens. Matter* **11**, 4539 (1999).